

Available online at https://jmeche.uitm.edu.my/browsejournals/special-issues/

Journal of Mechanical Engineering

Journal of Mechanical Engineering SI 14 2025, 110 – 127.

Multi-Objective Optimisation of Abrasive Water-Jet Parameters for Titanium Alloy using Box-Behnken Response Surface Methodology

Nurul Hayati Abdul Halim¹, Izdihar Tharazi^{1*}, Abdul Hakim Abdullah¹, Farrahshaida Mohd Salleh¹, Mohamad Firhan Morni¹, Afeeqa Puteri Marzuki¹, Muhammad Ilham Khalit²

¹Faculty of Mechanical Engineering, Universiti Teknologi MARA (UiTM), 40450 Shah Alam, Malaysia ²Department of Mechanical Engineering, School of Engineering, Bahrain Polytechnic, 33349 Isa Town, Kingdom of Bahrain

ARTICLE INFO

Article history: Received 01 October 2025 Revised 29 October 2025 Accepted 31 October 2025 Online first Published 15 November 2025

Keywords: Titanium alloy Abrasive water jet machining Box Behnken design Response surface material Analysis of variance

DOI: 10.24191/jmeche.v14i1.9071

ABSTRACT

Titanium alloy is widely used in aerospace, military, and biomedical industries due to its high tensile strength and toughness, even at extreme temperatures. However, its poor machinability presents challenges for conventional cutting methods. Abrasive water jet machining (AWJM) is widely utilised for processing such hard-to-machine materials. This study aims to optimise critical AWJM parameters, including abrasive flow rate (0.286 kg/min - 0.318 kg/min), traverse speed (2000 mm/min - 4000 mm/min), and stand-off distance (5 mm - 15 mm), for machining titanium alloy using Response Surface Methodology (RSM). A total of 17 experimental runs were conducted, and analysis of variance (ANOVA) was applied to evaluate the influence of the selected parameters on kerf width, surface roughness, and material removal rate (MRR). Scanning electron microscopy (SEM) was also employed to examine the surface defect pattern and microstructural characteristics on the machined surface. The results show that stand-off distance and traverse speed were the most significant factors affecting all three responses, with optimal values of 5 mm and 3000 mm/min, respectively. Increasing the stand-off distance led to higher values for all responses, while an increase in traverse speed produced the opposite trend. The abrasive flow rate was the least influential, with an optimal value of 0.318 kg/min. SEM analysis revealed surface defects such as garnet embedment, ploughing, and grooves under non-optimised conditions. The optimised parameters obtained can improve the machining quality and serve as a useful reference for future research and industrial applications.

^{1*} Corresponding author. E-mail address: izdihar92@uitm.edu.my https://doi.org/10.24191/jmeche.v14i1.9071

INTRODUCTION

Abrasive water jet machining (AWJM) has emerged as a versatile and energy-efficient alternative to conventional machining processes, particularly for hard-to-machine alloys and composites. The absence of continuous tool-workpiece contact in AWJM generates minimal heat, reduces tool wear, and enables the precise machining of temperature-sensitive and reflective materials. These attributes have made AWJM highly suitable for advanced engineering applications ranging from aerospace components and automotive prototypes to biomedical implants (Halim et al., 2024). In promoting sustainability, abrasive water jet machining (AWJM) supports efficient use of resources and the development of modern manufacturing systems. This aligns with the United Nations Sustainable Development Goal 9, which focuses on fostering industry, innovation, and infrastructure to achieve sustainable growth and technological progress in production sectors (Grieco & Palou-Rivera, 2020). Within the Malaysian context, this initiative is in harmony with the National Policy on Industry 4.0 (Industry4WRD) introduced by the Ministry of International Trade and Industry to encourage the integration of digital, low-waste, and intelligent machining practices across advanced manufacturing industries (Hasbullah & Abd Rahman, 2023).

One of the major challenges in AWJM is achieving high-quality surface finishes and dimensional accuracy, especially when machining titanium alloys. According to Kartal & Kaptan (2025), the process involves complex interactions between the target surface and the high-velocity abrasive—water jet, which commonly results in tapered kerfs, uneven edges, and poor geometric tolerances. These variations are caused by jet deflection, energy dispersion, and particle rebound effects that become worse as the stand-off distance and traverse speed increase (Wang et al., 2023). Similar optimization issues have been reported in other machining processes, such as CNC turning, where parameter interactions strongly influence surface integrity and roughness (Suhaimey et al., 2025; Mohamed et al., 2023). Thus, increasing dimensional accuracy is vital for producing parts that satisfy the high standards of biomedical and aerospace applications, where small geometrical changes can affect performance and safety standards.

The quality of AWJM-machined surfaces is mainly determined by process parameters such as traverse speed, abrasive flow rate (AFR), and stand-off distance (SOD). A lower stand-off distance reduces jet divergence, which improves cutting precision and produces smoother surfaces with smaller kerf widths. In contrast, a higher stand-off distance generally results in dimensional errors and jet energy losses (Fuse et al., 2025). Similarly, increasing traverse speed shortens the jet material interaction time, which decreases the material removal rate (MRR). However, higher traverse speeds also tend to deteriorate surface quality, resulting in a rougher surface and irregular cutting profiles (Abouzaid et al., 2024; Dekster et al., 2023). On the other hand, a moderate abrasive flow rate provides sufficient particle momentum for effective erosion, enhancing both material removal rate and surface uniformity. Excessive abrasive flow rate may cause turbulence and particle interference, leading to increased surface irregularities (Sami Abushanab et al., 2022). Therefore, it is important to achieve an optimal balance among these parameters, where the desired outcomes are higher MRR, lower surface roughness, and narrower kerf width, demonstrating enhanced machining quality and performance.

In this study, a titanium alloy was chosen as the workpiece. The choice is mainly because this material has a combination of good mechanical behaviour, which allows it to withstand high loads, stable at elevated temperatures, and does not corrode easily. Because of that, titanium alloys have become a popular option for critical components, especially in aircraft structures and engines. They are also commonly used for medical implant devices and certain electronic applications (Pushp et al., 2022). On the other hand, machining titanium is known to be troublesome. The material does not conduct heat well, and it hardens quickly during cutting. It also reacts easily under machining conditions. All of these issues reduce its machining performance and make common processes like milling, turning, and drilling much more challenging (Semenova et al., 2023).

The performance quality of AWJM processes is highly dependent on the precise adjustment of process parameters. Kolahan & Khajavi (2009) indicate that optimising AWJM performance is complex due to the interplay of physical phenomena and machine limitations. Stand-off distance, traverse speed, and abrasive flow rate are among the adjustable parameters, while pump pressure is typically held constant. These parameters collectively influence machining performance, like kerf width, surface roughness, and material removal rate (MRR). Moreover, AWJM is recognised as an environmentally sustainable process, as it generates minimal airborne pollutants, allows for water reuse, and offers the potential for abrasive recycling (Guglielmi et al., 2021).

Although AWJM offers many benefits, there is still a lack of detailed studies that consider how its main input parameters jointly affect kerf quality and the microstructural response of titanium alloys. In line with this gap, the present work aims to investigate how stand-off distance (SOD), traverse speed, and abrasive flow rate (AFR) influence kerf width, surface roughness, and material removal rate (MRR) when machining titanium alloy. To achieve this, Response Surface Methodology (RSM) based on a Box Behnken Design (BBD) was implemented to plan the trials and model the responses. BBD was selected because it reduces the number of required experiments and prevents extreme factor levels, which can be risky or unrealistic in machining tests (Tharazi et al., 2020). In addition, statistical analysis using analysis of variance (ANOVA) was employed to develop predictive models and to identify the most suitable combination of parameters that can enhance machining performance and surface integrity.

MATERIAL AND METHOD

Material and experimental setup of AWJM

In this study, the studied material was a (Ti-6Al-4V) titanium alloy plate Grade 5 with dimensions of 399 mm \times 61 mm \times 6.6 mm, and an average hardness of 340 HV (\pm 10 HV) as illustrated in Fig 1. Cutting operations were conducted to produce square-shaped specimens measuring 15 mm \times 15 mm using an abrasive water jet (AWJ) machine, Flow Mach 100 series. The system can move at speeds of up to 10 m/min, and its linear motion accuracy is maintained within approximately 0.13 mm for every metre of travel. Silica abrasive particles with a mesh size of 80 were employed as the cutting medium. Fig 2 presents the results of the cutting process, illustrating the square holes produced on the titanium alloy plate and the corresponding extracted specimens.

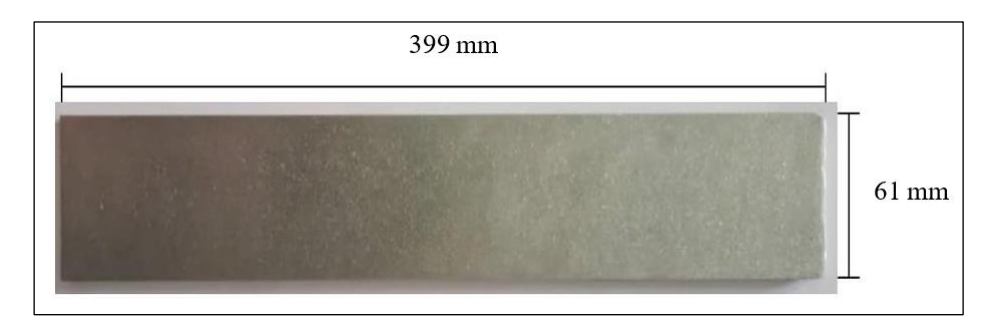


Fig. 1. Plate of titanium alloy.

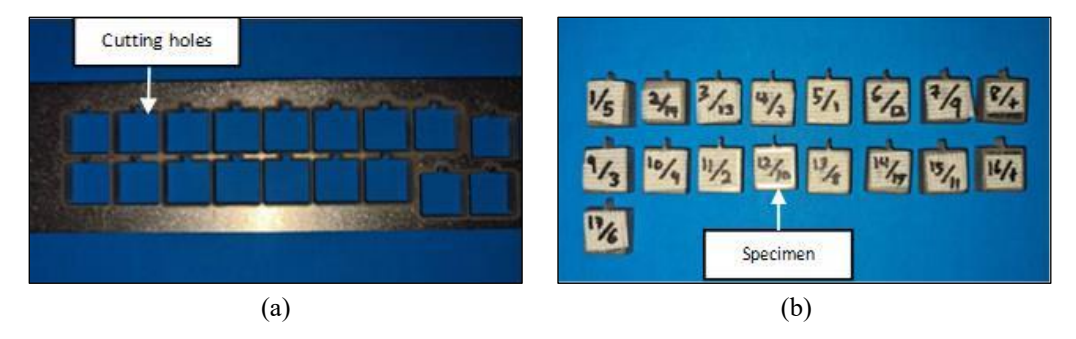


Fig. 2. The outcome of cutting operations (a) square holes and (b) the extracted specimen.

Design of experiment using Box-Behnken Design

A schematic diagram of the abrasive water jet machining setup (AJWM) is presented in Fig 3. The diagram illustrates the main process parameters investigated, namely the stand-off distance (SOD), traverse speed, and abrasive flow rate. The SOD refers to the vertical distance between the nozzle tip and the workpiece surface, which in the study ranged from 5 to 15 mm. The traverse speed corresponds to the linear motion of the nozzle across the workpiece, varied between 2000 mm/min and 4000 mm/min. the abrasive flow rate represents the mass of abrasive particles delivered through the nozzle, adjusted between 0.286 kg/min to 0.318 kg/min. Each parameter was varied across three levels, as shown in Table 1. These parameters and value ranges were selected based on preliminary trial runs, previous research, and the capabilities of the available AWJM machine to ensure stable jet cutting and measurable machining responses. The water jet pressure (379 MPa) and abrasive type (80 mesh silica) were kept constant throughout the experiments.

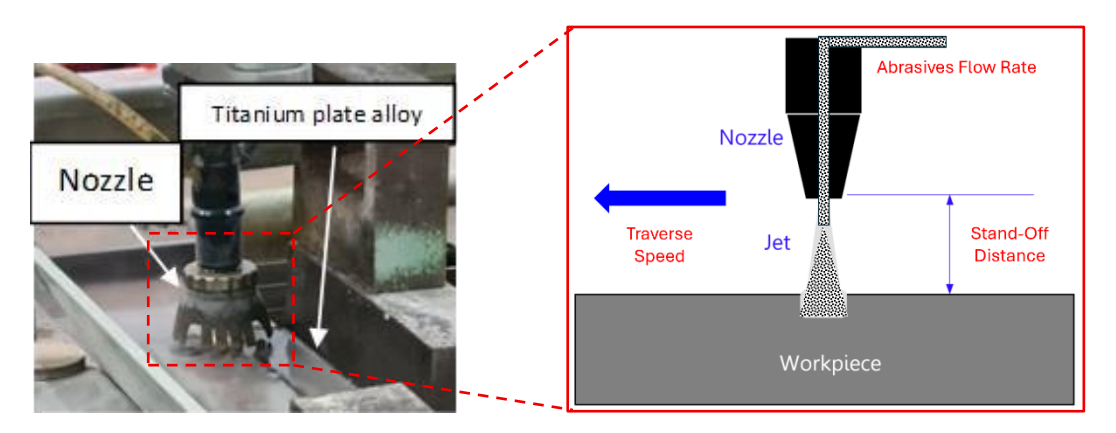


Fig. 3. Schematic representation of the abrasive water jet machining (AWJM) setup, illustrating the key process parameters: stand-off distance, traverse speed, and abrasive flow rate.

Table 1. Abrasive water jet machining parameters

Variable parameters	Unit	Level 1	Level 2	Level 3
Stand-off distance	mm	5	10	15
Traverse speed	mm/min	2000	3000	4000
Abrasive flow rate	kg/min	0.285	0.302	0.318

Here, the machining tests were planned using Response Surface Methodology (RSM). The Box-Behnken Design (BBD) was applied since it allows three factors to be tested at three levels, and this layout generated 17 runs. For each experiment, the kerf width, surface roughness, and material removal rate (MRR) were obtained for later analysis.

ANOVA was carried out to check which factors had a meaningful influence on the responses, as well as to observe any interaction effects between the parameters. Subsequently, the numerical optimisation function in Design Expert was used to identify the optimal combination of SOD, TS, and AFR for achieving desirable machining outcomes. In this optimisation study, the desired goals were set to minimise kerf width and surface roughness, while maximising the MRR to enhance productivity. These optimisation criteria guided the selection of the optimal process parameters in subsequent analyses.

The optimal machining parameter identified through ANOVA analysis was then validated experimentally using identical conditions. The corresponding responses, such as kerf width, surface roughness, and MRR, were measured following the same procedures. The percentage error between the experimental (actual) results and the predicted values from the regression model was calculated to evaluate the accuracy of the optimisation. Design Expert Version 13 software was used for experimental design, statistical analysis, and validation as confirmation of the reliability and effectiveness of the RSM parameter optimisation.

Characterisation of machining quality and surface morphology

Kerf width measurements were performed using a vernier calliper, as illustrated in Fig 4. Both the square holes and the corresponding square-shaped specimens were measured, and the kerf width was calculated as the difference between the dimensions of the square hole and those of the respective specimen. In addition to kerf width analysis, the study also examined the surface roughness of the vertical walls of the square-shaped specimens machined by abrasive water jet cutting. Surface roughness was measured using a Surftest SV-600 device, which is designed for assessing the topography of flat surfaces.

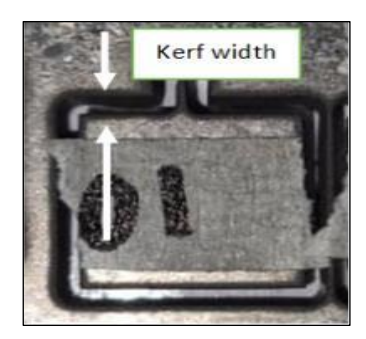


Fig. 4. Kerf width of specimen.

For this study, the MRR (mm³/min) was worked out by taking the volume of material removed and dividing it by the machining duration. Referring to Equation 1, the volume removed was estimated based on the overall cutting length generated by the AWJM process together with the kerf width and the cutting depth.

$$MRR = \frac{h (Depth \ of \ cut) \times w \ (Kerf \ width) \times l \ (Nozzle \ distance)}{t \ (Machining \ time)} \tag{1}$$

After the cutting trials were completed, the machined surfaces were observed using a Hitachi SU3500 scanning electron microscope (SEM). The morphological evaluation was performed on surfaces produced under non-optimised machining conditions, which involved parameter settings selected at the lowest, middle, and highest levels.

RESULTS AND DISCUSSION

Experimental results

Table 2 highlights the three primary output responses evaluated in this AWJM study, namely kerf width, surface roughness, and the material removal rate (MRR). All these responses were observed to change depending on the stand-off distance (SOD), traverse speed, and abrasive flow rate (AFR) that were applied during machining. From the results obtained, it can be clearly seen that reducing SOD from 15 mm down to 5 mm continuously produced smaller kerf widths. A comparable trend was also detected when the traverse speed was raised from 2000 mm/min to 4000 mm/min, where a higher cutting speed also helped to narrow down the kerf. These effects become most obvious when looking at runs 4, 5, and 13. Under these specific test conditions, the kerf width was found to be around 0.74 mm - 0.75 mm when the SOD was set to 5 mm, together with a high traverse speed of 4000 mm/min. On the contrary, run 2 produced the widest kerf, which was approximately 1.10 mm. This occurred when the SOD was at its highest level of 15 mm and the traverse speed was at the slowest setting of 2000 mm/min. These trends agree well with established behaviour reported in the AWJM literature. A larger SOD typically causes the jet to diverge more before reaching the surface, resulting in lower cutting energy density and more energy loss, which then allows the kerf to expand laterally. In contrast, when the traverse speed is increased, the contact duration between the abrasive jet and the workpiece surface becomes shorter. This reduces the material removal interaction time and therefore limits side material erosion, which ultimately helps to suppress excessive kerf enlargement (Abouzaid et al., 2024; Mohamad et al., 2020; Rowe et al., 2023).

Surface roughness exhibits a similar SOD, with a dependent pattern. Average surface roughness values remain below 1.90 μ m at SOD of 5 mm (runs 9 - 11) but increase to approximately 2.0 μ m when the SOD is raised to 15 mm (runs 2, 3, 6, and 14). This deterioration in surface quality can be minimised by increasing traverse speed. For example, run 6 achieves a lower surface roughness (4000 mm/min, 2.07 μ m) than run 3 (3000 mm/min, 2.03 μ m) at identical SOD, indicating that reduced exposure time limits micro-chipping and striation development. These observations support previous findings that surface roughness increases with higher stand-off distances due to jet spreading, and at low traverse speeds because of reduced kinetic energy, which leads to uneven cutting and small cracks on the cut surface (Pahuja et al., 2019; Sami Abushanab et al., 2022).

The MRR ranges from 4.58 mm³/s to 6.91 mm³/s and is influenced by the opposing effects of traverse speed and abrasive flow rate. Although the theoretical relation MRR \propto (feed length) \times (kerf width) \times (depth of cut) indicates that higher traverse speed can enhance productivity, runs 4 and 5 demonstrate that the associated reduction in kerf width may limit the benefit, resulting in lower MRR values compared to runs 1 and 3, despite the higher traverse speeds. In contrast, increasing AFR from 0.286 kg/min to 0.318 kg/min (run 11 vs. run 9) consistently improves MRR by increasing abrasive particle density and thus the erosive mass flux. Similar opposing and supporting effects of traverse speed and AFR have been reported in previous AWJM optimisation studies involving aerospace alloys (Llanto et al., 2021; Ramakrishnan, 2022; Tripathi et al., 2019). Overall, the data validate the Box-Behnken optimization approach, with the most balanced performance by a moderate kerf width (0.83 mm), low surface roughness (1.9 μ m), and high MRR (6.2 mm³/s), achieved at SOD of 5 mm, traverse speed of 3000 mm/min, and AFR of 0.318 kg/min (run 11).

Table 2. Results of kerf width, surface roughness, and material removal rate (MRR)

Run	Stand-off distance	Traverse speed	Abrasive flow rate	Kerf width	Surface roughness	MRR
Kun	(mm)	(mm/min)	(kg/min)	(mm)	(µm)	(mm^3/s)
1	10	3000	0.302	0.85	1.98	6.23
2	15	2000	0.302	1.10	1.91	6.22
3	15	3000	0.286	0.96	2.03	6.91
4	10	4000	0.286	0.74	1.98	5.64
5	5	4000	0.302	0.74	1.89	5.75
6	15	4000	0.302	0.81	2.07	6.29
7	10	2000	0.318	0.87	2.00	5.74
8	10	3000	0.302	0.93	2.01	6.82
9	5	3000	0.286	0.82	1.85	5.90
10	5	2000	0.302	0.81	1.75	4.58
11	5	3000	0.318	0.83	1.89	6.2
12	10	3000	0.302	0.85	2.01	6.23
13	10	4000	0.318	0.75	1.97	5.82
14	15	3000	0.318	0.85	1.92	6.35
15	10	2000	0.286	1.01	1.90	4.99
16	10	3000	0.302	0.93	2.08	6.82
17	10	3000	0.302	0.85	2.03	6.23

Analysis of kerf width

Table 3 demonstrates that the ANOVA results for kerf width exhibit strong statistical validity (F = 13.44, p = 0.0003). Among the process variables, the traverse speed is identified as the most influential factor (F = 42.94, p < 0.0001), followed by stand-off distance (SOD) (F = 20.64, p = 0.0111). In contrast, the abrasive flow rate (AFR) exhibits a minimal effect at the 95 % confidence level (F = 4.04, p = 0.0722). The significant interaction between SOD and traverse speed (F = 7.39, p = 0.0216) shows that simultaneous optimisation of these parameters results in more accurate kerf-width control compared to individual adjustment. The findings align with previous studies on abrasive water jet machining, which report that lower SOD and traverse speed values result in a narrower kerf width, while the AFR has a lesser impact (Abouzaid et al., 2024; Tharazi et al., 2024).

Table 3. ANOVA results of kerf width

Source	Sum of squares	df	Mean square	F-value	P-value	
Model	0.1320	6	0.0220	13.44	0.0003	significant
A-Stand-off distance	0.0338	1	0.0338	20.64	0.0011	
B-Traverse speed	0.0703	1	0.0703	42.94	< 0.0001	
C-Abrasive flowrate	0.0066	1	0.0066	4.04	0.0722	
AB	0.0121	1	0.0121	7.39	0.0216	
AC	0.0036	1	0.0036	2.20	0.1689	
BC	0.0056	1	0.0056	3.44	0.0935	
Residual	0.0164	10	0.0016			
Lack of Fit	0.0087	6	0.0014	0.7546	0.6397	not significant
Pure error	0.0077	4	0.0019			
Cor total	0.1484	16				
Std. dev.	Mean	C.V.%	R ²	Adjusted R ²	Predicted R ²	Adeq precision
0.0405	0.8647	4.68	0.8897	0.8235	0.6810	12.2278

https://doi.org/10.24191/jmeche.v14i1.9071

The regression model further exhibits a high coefficient of determination ($R^2 = 0.8897$; adjusted $R^2 = 0.8235$), a low coefficient of variation (4.68%), and an adequate precision of 12.23, indicating that the model's reliability and its ability to accurately represent the fundamental process behaviour within the experimental range through the response surface method. Additionally, the non-significant lack of fit test (p = 0.6397) indicates the absence of systematic error, while the low standard deviation (0.0405) reflects a good repeatability of the experimental data. The statistics presented fulfil the criteria of response-surface methodology, thereby validating the use of the Box–Behnken design in modelling kerf width as a function of SOD, traverse speed, and AFR in abrasive water jet machining (Deaconescu & Deaconescu, 2021). A mathematical model developed based on the ANOVA results in Table 3 is given by Equation 2.

$$Kerf\ width = 0.864706 + 0.065 * A - 0.09375 * B - 0.02875 * C - 0.055 * AB - 0.03 * AC + 0.0375 * BC$$
(2)

Fig 5 provides further support for the model validation. The normal probability plot shows a line that is almost straight, which suggests that the residuals are randomly scattered and follow a behaviour close to a normal distribution. This indicates that the model assumptions are reasonably satisfied. In addition, the predicted-versus-actual plot also confirms the strength of the developed model, as most of the plotted points are located close to the 45° reference line. When the predicted and measured values fall near this diagonal line, it shows that the model is capable of producing estimates that are highly comparable to the actual experimental data. Hence, both plots collectively verify that the predictive performance of the model is acceptable and reliable.

Fig 6 depicts the three-dimensional response surface for kerf width in relation to SOD and traverse speed, with the AFR held constant. Kerf width increases consistently towards the high SOD and low traverse speed region, indicating that increasing SOD and decreasing traverse speed both contribute to a wider cut. This observation is consistent with prior findings that higher SOD leads to greater jet divergence and energy dissipation, while a slower traverse speed enhances jet-material contact time, collectively resulting in larger kerf width values (Krajcarz et al., 2017; Mohamad et al., 2020). The contour projection indicates that maintaining SOD around 5 mm and a traverse speed above approximately 3500 mm/min limits kerf width below 0.80 mm. This supports optimisation studies that recommend low SOD and high traverse speed settings for achieving precise cutting without compromising productivity (Abouzaid et al., 2024; Rowe et al., 2023).

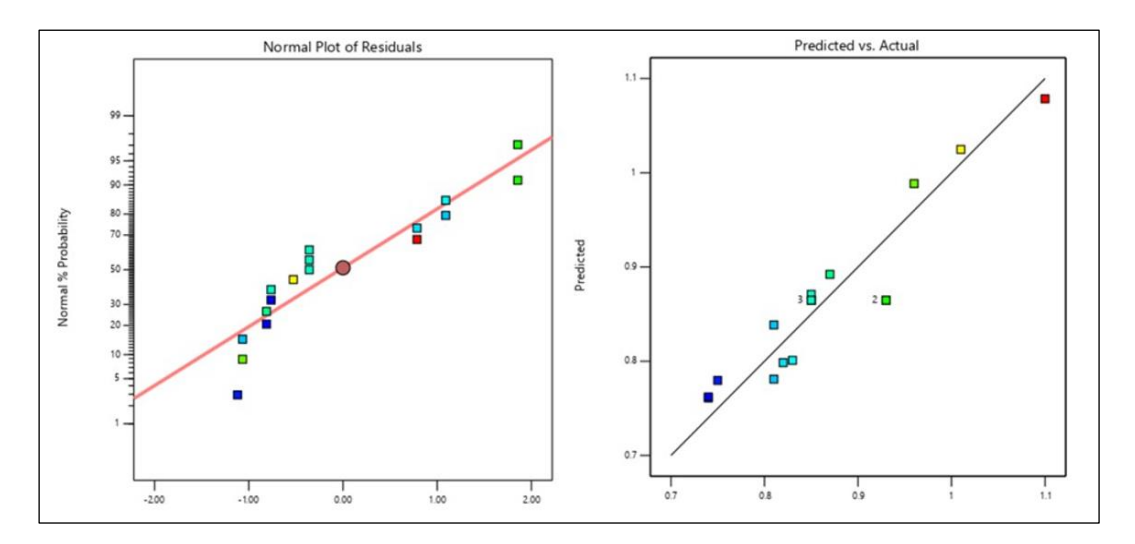


Fig. 5. Residual and prediction plots for model validation of kerf width. https://doi.org/10.24191/jmeche.v14i1.9071

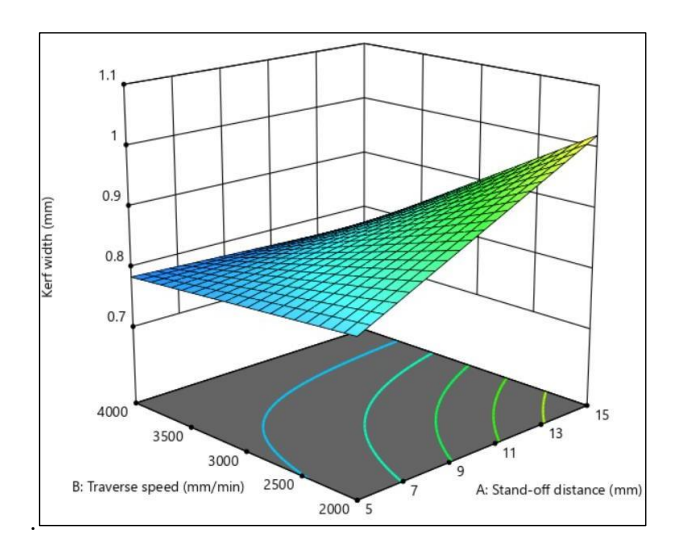


Fig. 6. The 3D surface of kerf width.

Analysis of surface roughness

Table 4 shows that the ANOVA results for surface roughness are statistically meaningful (F = 9.84, p = 0.0012). Among the three input variables, the stand-off distance (SOD) is clearly the dominant factor influencing surface finish, as reflected by the highest F-value (F = 13.70, p = 0.0027). The next most influential parameter is traverse speed (F = 5.55, p = 0.0349). In addition, the significant quadratic term for SOD (A^2 , p = 0.0069) reveals the presence of a curved response trend rather than a purely linear relationship. Furthermore, the lack-of-fit value (p = 0.1996) is not significant, which indicates that the developed model is appropriate and capable of representing the experimental data reasonably well. Overall, the observed patterns are in line with earlier research on abrasive water jet machining. Generally, when the SOD is increased and the traverse speed is lowered, the surface roughness tends to become worse because of prolonged jet impact and additional material erosion. Meanwhile, AFR appears to have only a modest or negligible effect on the surface finish response, which has also been reported in previous studies (Hascalik et al., 2007; Sami Abushanab et al., 2022).

Table 4. ANOVA result of surface roughness

Source	Sum of squares	df	Mean square	F-value	p-value	
Model	0.0815	3	0.0272	9.84	0.0012	significant
A-Stand-off distance	0.0378	1	0.0378	13.70	0.0027	
B-Traverse speed	0.0153	1	0.0153	5.55	0.0349	
A^2	0.0283	1	0.0283	10.27	0.0069	
Residual	0.0359	13	0.0028			
Lack of fit	0.0304	9	0.0034	2.47	0.1996	not significant
Pure error	0.0055	4	0.0014			
Cor total	0.1174	16				
Std. dev.	Mean	C.V. %	R ²	Adjusted R ²	Predicted R ²	Adeq precision
0.0525	1.96	2.68	0.6942	0.6236	0.4670	9.3409

The coefficients of determination for the model are $R^2 = 0.6942$ and adjusted $R^2 = 0.6236$, with an adequate precision of 9.34, demonstrating a reliable and statistically validated model performance within https://doi.org/10.24191/jmeche.v14i1.9071

the experimental range. The predicted R^2 (0.4670) is in close agreement with the adjusted R^2 , and the low coefficient of variation (2.68%) indicates consistency of the model developed through response surface methodology (Fuse et al., 2025). Equation 3 presents the mathematical model obtained from the regression analysis of surface roughness.

$$Surface\ roughness = 1.99556 + 0.06875 * A + 0.04375 * B - 0.0818056 * A2$$
 (3)

Fig 7 supports these findings, as the normal probability plot of residuals demonstrates an approximately linear trend, indicating that the residuals follow a normal distribution. Meanwhile, the predicted versus actual plot reveals that most data points are closely grouped around the 45° line, confirming a strong correlation between actual and predicted surface roughness values.

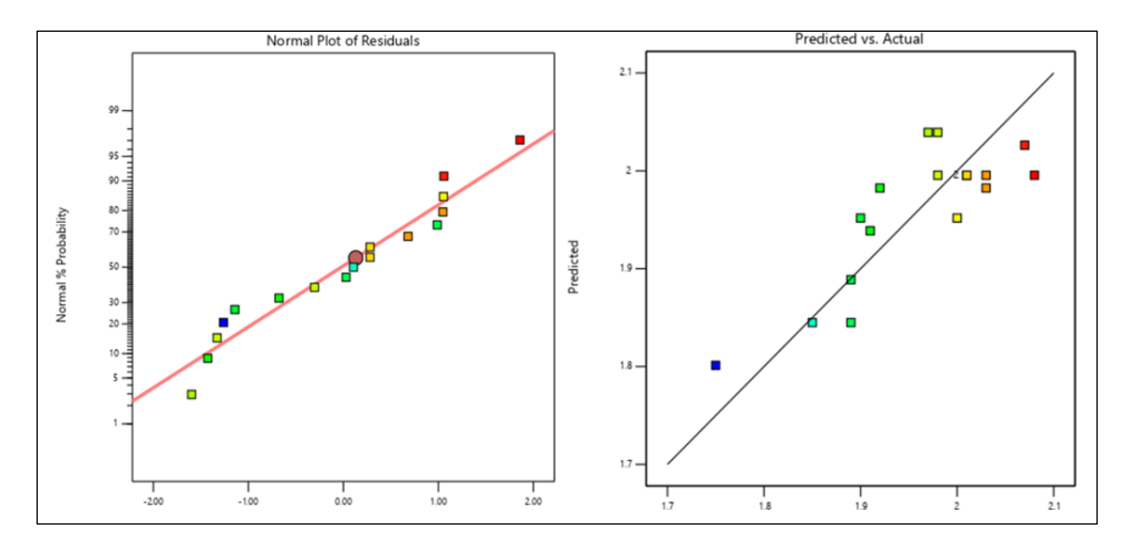


Fig. 7. Residual and prediction plots for model validation of surface roughness.

The three-dimensional surface depicted in Fig 8 illustrates that surface roughness increases significantly when the SOD exceeds approximately 12 mm and the traverse speed drops below 2500 mm/min. In contrast, maintaining the SOD between 5 mm and 8 mm and a traverse speed above 3500 mm/min results in surface roughness below 1.9 μ m. The notable curvature along the SOD axis confirms the significance of its quadratic term, while the mild slope along the traverse-speed axis indicates a less dominant yet influential contribution. This optimal parameter supports previous optimisation studies that recommend low SOD and high traverse speed to enhance surface integrity in abrasive water jet machining of titanium alloys (Rowe et al., 2023).

Analysis of material removal rate

Table 5 indicates that the regression model for material removal rate (MRR) is statistically significant (F = 9.59, p = 0.0010). Among the primary factors, stand-off distance (SOD) exhibits the most significant linear effect (F = 11.83, p = 0.0049), whereas traverse speed shows a minor main-effect contribution (F = 4.12, p = 0.0652). The abrasive flow rate (AFR) is not statistically significant at the 95 % confidence level (p = 0.5033). The significance of the quadratic term for traverse speed (B², F = 21.94, p = 0.0005) reveals curvature in the response, demonstrating that excessively high traverse speed ultimately results in decreasing efficiency in MRR. The non-significant lack of fit test (p = 0.4623) and adequate precision of

10.55 (above the minimum limit of 4) confirm that the model is both reliable and predictive, in agreement with criteria for response surface methodology studies.

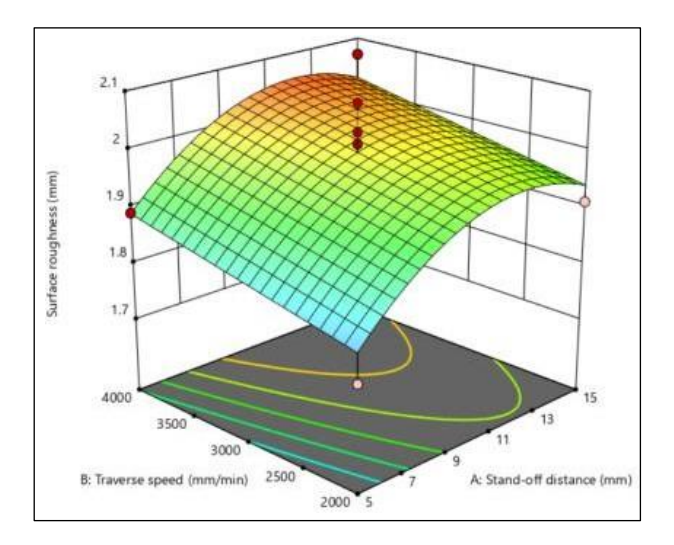


Fig. 8. The 3D surface of surface roughness.

Table 5. ANOVA result of the material removal rate (MRR)

Source	Sum of squares	df	Mean square	F-value	p-value	
Model	4.52	4	1.13	9.59	0.0010	significant
A-Stand-off distance	1.39	1	1.39	11.83	0.0049	
B-Traverse speed	0.4851	1	0.4851	4.12	0.0652	
C-Abrasive flowrate	0.0561	1	0.0561	0.4762	0.5033	
B^2	2.59	1	2.59	21.94	0.0005	
Residual	1.41	12	0.1178			
Lack of fit	0.9963	8	0.1245	1.19	0.4623	not significant
Pure error	0.4177	4	0.1044			
Cor total	5.93	16				
Std. dev.	Mean	C.V. %	R ²	Adjusted R ²	Predicted R ²	Adeq precision
0.3433	6.04	5.68	0.7617	0.6823	0.4912	10.4545

The coefficient of variation is low at 5.68 % and the difference between adjusted R² (0.6823) and predicted R² (0.4912) is within the acceptable limit of 0.2. Additionally, the standard deviation remains relatively low at 0.0525. These statistical outputs verify that MRR can be reliably modelled as a function of SOD, traverse speed, and AFR within the experimental parameter range (Sai et al., 2023). Based on the ANOVA results for MRR, the corresponding mathematical model is presented in Equation 4.

$$MRR = 6.41 + 0.4175 * A \ 0.24625 * B + 0.08375 * C - 0.275 * AB - 0.78125 * B^{2}$$
 (4)

Fig 9 supports the statistical validity of the model. The normal probability plot of residuals displays an approximately linear trend, indicating that the residuals follow a normal distribution. The predicted versus

actual plot shows most data grouping near the 45° reference line, demonstrating a strong predictive accuracy.

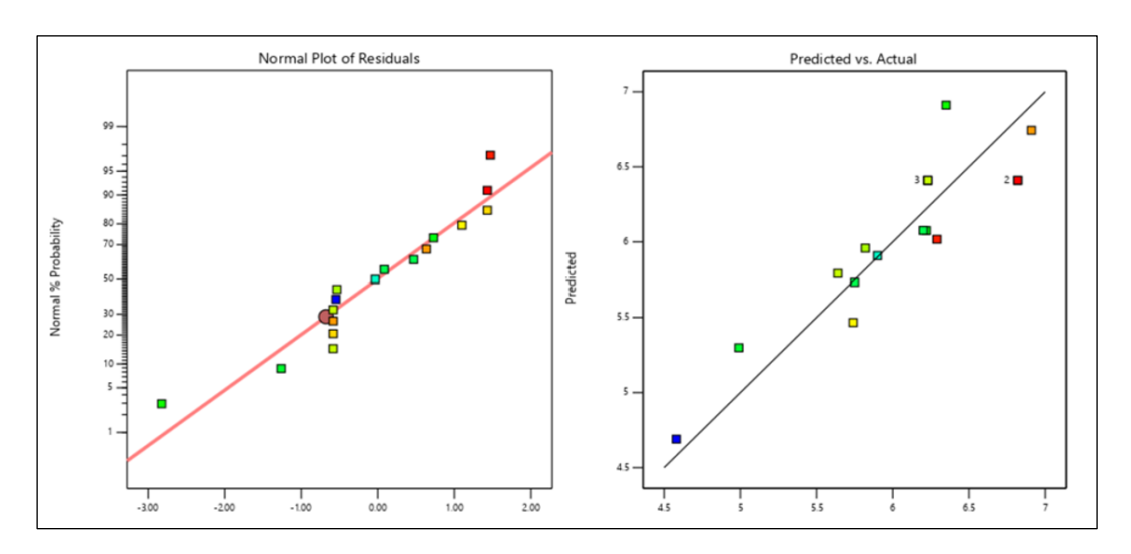


Fig. 9. Residual and prediction plots for model validation of material removal rate (MRR).

The three-dimensional response surface in Fig 10 shows that MRR increases significantly when traverse speed rises from 2000 mm/min to approximately 3500 mm/min, provided that the SOD remains within the range between 8 mm and 12 mm. Beyond this point, the MRR tends to plateau, aligning with the previous studies that report moderate SOD allows efficient jet penetration, while higher traverse speed enhances volumetric removal without inducing excessive jet dispersion (Dekster et al., 2023; Perumal et al., 2023). At higher SOD values (> 13 mm), MRR begins to decrease due to the expansion of the jet footprint, which reduces energy density at the impact site. In contrast, at very low SOD values (< 6 mm), the restricted working distance limits slurry acceleration, resulting in lower MRR despite high traverse speed. The surface contours therefore define the optimal operating parameters, SOD around 10 mm and traverse speed near 3500 mm/min, where MRR reaches approximately 6.9 mm³/s without negatively affecting surface roughness or kerf width. These findings serve as a reference for the practical optimisation of abrasive water jet machining of titanium alloys.

Microstructure analysis

The cross-sectional examination of the machined surface was conducted to observe surface defects resulting from abrasive water jet machining (AWJM). This investigation was carried out using non-optimised process parameters at three levels: (a) minimum, (b) medium, and (c) maximum settings on titanium alloy specimens. The SEM images were captured from the machined surface area at the midsection of the kerf, where erosion and defect formation are most significant due to direct jet impingement. Fig 11 presents the SEM images of the tested specimens: (a) SOD: 5 mm, traverse speed: 2000 mm/min, abrasive flow rate: 0.302 kg/min; (b) SOD: 10 mm, traverse speed: 3000 mm/min, abrasive flow rate: 0.302 kg/min. Surface defects such as garnet embedment, ploughing, and grooves were observed, particularly under high stand-off distance and traverse speed conditions.

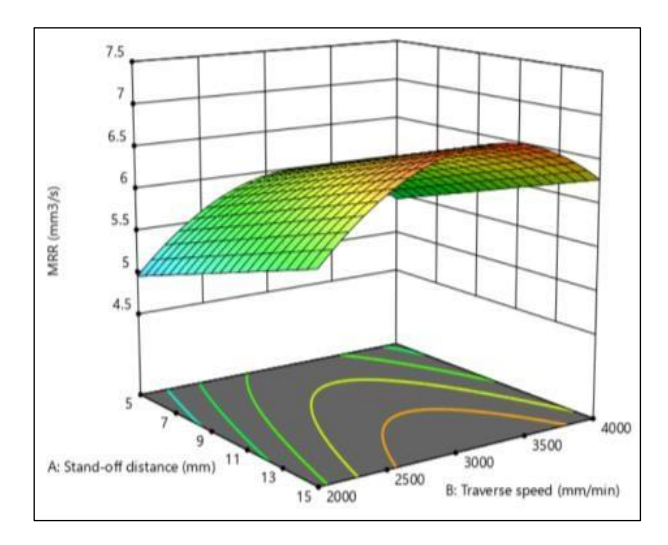


Fig. 10. The 3D surface of material removal rate (MRR).

Fig 11(a) indicates that samples cut at lower traverse speed show fewer embedded garnet particles compared to those machined at higher traverse speed. This observation suggests that when the cutting head moves slowly, each abrasive particle spends more time interacting with the surface, which allows it to remove material more effectively rather than becoming lodged in the workpiece. On the other hand, at higher traverse speeds, the jet tends to become more unstable. The collision between the forward jet stream and the rebound jet creates turbulence, which may force abrasive particles to become trapped and embedded in the machined wall instead of removing material efficiently (Lenin Raj & Rajadurai, 2019).

In addition, ploughing marks were observed on all three surfaces examined, implying that the abrasive particles experienced a reduction in their kinetic energy as the cutting progressed. When the particle velocity decreases, the erosive cutting mechanism becomes weaker, and the tool-path transitions more towards deformation and ploughing. Prior work has shown that fractured or irregular-shaped abrasives often generate more ploughing due to their unstable and inconsistent impact geometry, while spherical abrasives tend to glide or roll on the surface, thus contributing to less effective cutting (Umanath et al., 2021)

Further support can be seen in Figs 11(b) and 11(c). Deep grooves are present on the machined surfaces, which can be linked to the strong and repeated impact of sharp-edged particles on the titanium substrate (Tharazi et al., 2024). This behaviour aligns well with the erosive wear theory in AWJM, which states that sharper particles strike with concentrated force and remove material through micro-chipping. Therefore, the interplay between traverse speed, particle shape, and jet stability directly influences whether the abrasive acts as a cutting agent or becomes embedded in the surface. These insights highlight the importance of optimising traverse speed and controlling abrasive morphology to minimise undesirable embedment and improve the final surface integrity.

Experiment validation

The main aim of this research was to determine the most suitable combination of machining parameters when cutting titanium alloy using the abrasive water jet machining (AWJM) process. To achieve this, a statistical optimisation approach was applied, where both ANOVA and Response Surface Methodology (RSM) were utilised to study how the input factors contribute to the measured outputs, and to mathematically predict the best conditions. The analysis carried out through this optimisation procedure revealed that the most favourable parameter setting corresponds to operating the machine at a relatively low stand-off distance (5 mm), together with a moderate traverse speed (3000 mm/min), and a https://doi.org/10.24191/jmeche.v14i1.9071

comparatively high abrasive feed rate (0.318 kg/min). These specific settings generated the best compromise between material removal efficiency and surface quality. A complete summary of these optimum values can be found in Table 6, and the results demonstrate that proper balancing of these three parameters is crucial to maximise AWJM performance for titanium alloys.

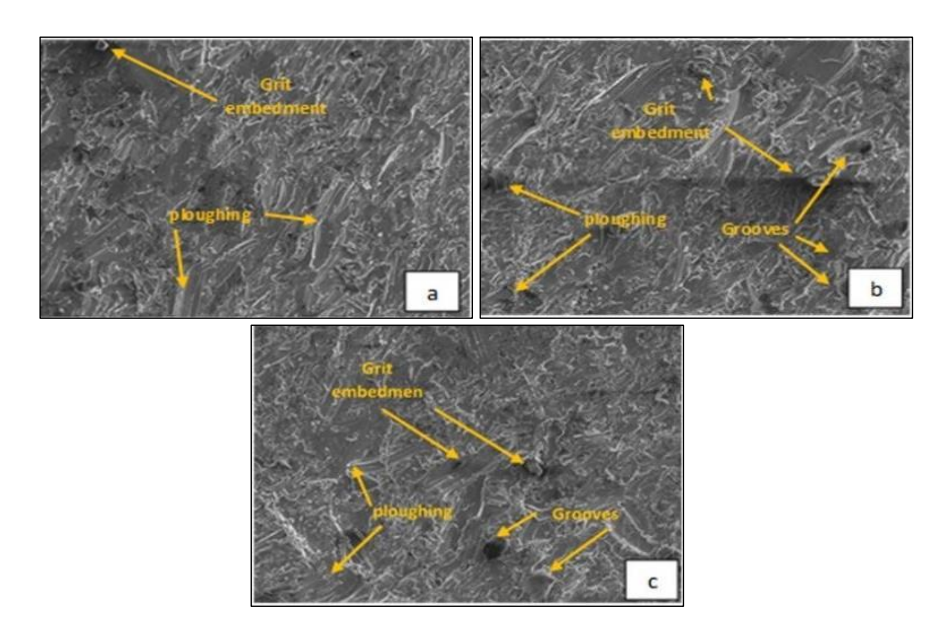


Fig. 11. Surface defects at three levels of process parameter (a) minimum, (b) medium and (c) maximum.

Table 6. Optimized parameters of AWJM

Stand-off distance (mm)	Traverse Speed (mm/min)	Abrasive flow rate (kg/min)
5	3000	0.318

Machining trials were subsequently performed under these optimal conditions, and the resulting kerf width, surface roughness, and material removal rate (MRR) were experimentally measured. The predicted values for each response were obtained using the regression models developed in Equations 2-4, which were previously validated through ANOVA. The actual value (ν A) refers to the result obtained experimentally using the optimal machining parameters, while the expected value (ν E) represents the predicted outcome generated through optimisation using Design-Expert software. The accuracy of the models was evaluated by comparing these actual and predicted values, and the percentage error for each response was calculated using Equation 5.

$$Percentage\ error = \frac{|vA - vE|}{vE} \ x \ 100 \tag{5}$$

As shown in Table 7, the percentage errors for kerf width, surface roughness, and MRR were 6.11%, 2.9%, and 0.72%, respectively, demonstrating alignment with the accepted maximum of 10% (Halim et al., 2019). These results confirm the reliability of the developed models and the effectiveness of the optimisation method. The minimal difference between experimental and predicted values indicates that the proposed modelling and optimisation approach successfully demonstrated an accurate representation of the process response, aligning with the objective of the study.

https://doi.org/10.24191/jmeche.v14i1.9071

Table 7. Percentage of error according to the response of optimized parameters

	Kerf width (mm)	Surface roughness (µm)	Material removal rate (mm ³ /s)
Actual value (v _A)	0.85	1.9	6.12
Expected value (vE)	0.801	1.845	6.076
Percentage error (%)	6.11	2.9	0.72

CONCLUSION

In conclusion, this study successfully applied the Box-Behnken experimental design to develop and evaluate the abrasive water jet (AWJ) cutting process for titanium alloy material. The investigation involved 17 machining trials, where the stand-off distance (SOD), traverse speed, and abrasive flow rate (AFR) were systematically varied to examine their influence on machining performance. The ANOVA outcomes confirmed that SOD and traverse speed were the two dominant parameters affecting the main responses, namely surface roughness, kerf width, and material removal rate (MRR). In contrast, AFR showed a comparatively minor effect on these responses. The surface morphology observations obtained from SEM further supported these findings. Specimens machined under unfavourable or non-optimised conditions clearly exhibited surface-related defects, including abrasive embedment, ploughing deformation, and distinct groove formation. These features highlight that parameter selection is crucial in AWJ machining, as inappropriate settings may reduce cutting efficiency and degrade surface quality. Based on the overall optimisation results, the recommended settings for producing favourable machining outcomes on Ti-6Al-4V are a low SOD of 5 mm, a medium traverse speed of 3000 mm/min, and a high AFR of 0.318 kg/min. These parameters showed the best balance between minimising kerf width, improving surface finish, and increasing MRR. The study therefore reinforces the capability and versatility of AWJ as a machining technique, especially for materials that are difficult to process using traditional cutting systems. For future work, additional responses such as taper angle, dimensional accuracy, or subsurface integrity could be included to broaden the performance evaluation. Further investigations on other controllable input variables, including water pressure, abrasive mesh size, abrasive type, and nozzle wear, are also recommended to further expand the knowledge base and strengthen the practical applicability of AWJ technology in advanced manufacturing.

ACKNOWLEDGEMENTS

The authors would like to acknowledge the support of the Faculty of Mechanical Engineering, Universiti Teknologi MARA, Shah Alam, Selangor, Malaysia, for providing the facilities and financial support for this research.

CONFLICT OF INTEREST

Two of the authors, Izdihar Tharazi and Nurul Hayati Abdul Halim are the Assistant Manging Editors and the Section Editor of the Journal Mechanical Engineering (JMeche), respectively. The authors have no other conflicts of interest to note.

AUTHORS' CONTRIBUTIONS

The authors confirm the equal contribution in each part of this work. All authors reviewed and approved the final version of this work.

REFERENCES

- Abouzaid, A., Mousa, S., & Ibrahim, A. M. M. (2024). Effect of standoff distance and traverse speed on the cutting quality during the abrasive water jet machining (AWJM) of brass. Machining Science and Technology, 28(3), 392–414. https://doi.org/10.1080/10910344.2024.2332874
- Deaconescu, A., & Deaconescu, T. (2021). Response surface methods used for optimization of abrasive waterjet machining of the stainless steel X2 CrNiMo 17-12-2. Materials, 14(10), 2475. https://doi.org/10.3390/ma14102475
- Dekster, L., Karkalos, N. E., Karmiris-Obratański, P., & Markopoulos, A. P. (2023). Evaluation of the machinability of Ti-6Al-4V titanium alloy by AWJM using a multipass strategy. Applied Sciences, 13(6), 3774. https://doi.org/10.3390/app13063774
- Fuse, K., Vora, J., Wakchaure, K., Patel, V. K., Chaudhari, R., Saxena, K. K., Bandhu, D., & Ramacharyulu, D. A. (2025). Abrasive waterjet machining of titanium alloy using an integrated approach of taguchibased passing vehicle search algorithm. International Journal on Interactive Design and Manufacturing, 19(3), 2249–2263. https://doi.org/10.1007/s12008-024-01831-0
- Grieco, B., & Palou-Rivera, I. (2020). Achieving sustainable development goals. Advanced manufacturing progress. CEP Magazine.
- Guglielmi, G., Mitchell, B., Song, C., Kinsey, B. L., & Mo, W. (2021). Life cycle environmental and economic comparison of water droplet machining and traditional abrasive waterjet cutting. Sustainability, 13(21), 12275. https://doi.org/10.3390/su132112275
- Halim, N. H. A., Haron, C. H. C., Ghani, J. A., & Azhar, M. F. (2019). Prediction of cutting force for milling of Inconel 718 under cryogenic condition by response surface methodology. Journal of Mechanical Engineering, 16(1), 1–16. https://doi.org/10.24191/jmeche.v16i1.6030
- Halim, N. H. A., Tharazi, I., Salleh, F. M., Morni, M. F., Khalit, M. I., & Abdullah, M. A. A. (2024). Multi-objectives optimization of abrasive water jet machining (AJWM) on mild steel. International Journal of Integrated Engineering, 16(5), 187–200. https://doi.org/10.30880/ijie.2024.16.05.015
- Hasbullah, A., & Abd Rahman. (2023). Industry4WRD. Ministry of Investment, Trade and Industry. https://www.miti.gov.my/index.php/pages/view/4832
- Hascalik, A., Çaydaş, U., & Gürün, H. (2007). Effect of traverse speed on abrasive waterjet machining of Ti-6Al-4V alloy. Materials & Design, 28(6), 1953–1957. https://doi.org/10.1016/j.matdes.2006.04.020
- Kartal, F., & Kaptan, A. (2025). Comprehensive and essential review of advanced researches abrasive waterjet machining. International Advanced Researches and Engineering Journal, 9(1), 50–69. https://doi.org/10.35860/iarej.1582470
- Kolahan, F., & Khajavi, A. H. (2009). Modeling and optimization of abrasive waterjet parameters using regression analysis. International Journal of Mechanical and Mechatronics Engineering, 3(11), 1425–1430.

- Krajcarz, D., Bańkowski, D., & Młynarczyk, P. (2017). The effect of traverse speed on kerf width in AWJ cutting of ceramic tiles. Procedia Engineering, 192, 469–473. https://doi.org/10.1016/j.proeng.2017.06.081
- Lenin Raj, S., & Rajadurai, A. (2019). Experimental study on deep-hole making in Ti-6Al-4V by abrasive water jet machining. Materials Research Express, 6(6), 066532. https://doi.org/10.1088/2053-1591/ab0c35
- Llanto, J. M., Tolouei-Rad, M., Vafadar, A., & Aamir, M. (2021). Impacts of traverse speed and material thickness on abrasive waterjet contour cutting of austenitic stainless steel AISI 304L. Applied Sciences, 11(11), 4925. https://doi.org/10.3390/app11114925
- Mohamad, W. N. F., Kasim, M. S., Norazlina, M. Y., Hafiz, M. S. A., Izamshah, R., & Mohamed, S. B. (2020). Effect of standoff distance on the kerf characteristic during abrasive water jet machining. Results in Engineering, 6, 100101. https://doi.org/10.1016/j.rineng.2020.100101
- Mohamed, F., Brahim, F., Toufik, B., & Mohamed Athmane, Y. (2023). Optimization and mathematical modelling of surface roughness criteria and material removal rate when milling C45 steel using RSM and desirability approach. Journal of Mechanical Engineering, 20(3), 173-197. https://doi.org/10.24191/jmeche.v20i3.23907
- Pahuja, R., Ramulu, M., & Hashish, M. (2019). Surface quality and kerf width prediction in abrasive water jet machining of metal-composite stacks. Composites Part B: Engineering, 175, 107134. https://doi.org/10.1016/j.compositesb.2019.107134
- Perumal, A., Kailasanathan, C., Wilson, V. H., Sampath Kumar, T., Stalin, B., & Rajkumar, P. R. (2023). Machinability of titanium alloy 6242 by AWJM through Taguchi method. Materials Today: Proceedings, 81(2), 606–611. https://doi.org/10.1016/j.matpr.2021.04.067
- Pushp, P., Dasharath, S. M., & Arati, C. (2022). Classification and applications of titanium and its alloys. Materials Today: Proceedings, 54(2), 537–542. https://doi.org/10.1016/j.matpr.2022.01.008
- Ramakrishnan, S. (2022). Investigating the effects of abrasive water jet machining parameters on surface integrity, chemical state in machining of Ti-6Al-4V. Materials Today Communications, 31, 103480. https://doi.org/10.1016/j.mtcomm.2022.103480
- Rowe, A., Pramanik, A., Basak, A. K., Prakash, C., Subramaniam, S., Dixit, A. R., & Radhika, N. (2023). Effects of abrasive waterjet machining on the quality of the surface generated on a carbon fibre reinforced polymer composite. Machines, 11(7), 749. https://doi.org/10.3390/machines11070749
- Sai, D. A., Nataraj, K. S., & Lakshmana, R. A. (2023). Response surface methodology-a statistical tool for the optimization of responses. Global Journal of Addiction & Rehabilitation Medicine, 7(1), 555705. https://doi.org/10.19080/gjarm.2023.07.555705
- Sami Abushanab, W., Moustafa, E. B., Harish, M., Shanmugan, S., & Elsheikh, A. H. (2022). Experimental investigation on surface characteristics of Ti6Al4V alloy during abrasive water jet machining process. Alexandria Engineering Journal, 61(10), 7529–7539. https://doi.org/10.1016/j.aej.2022.01.004
- Semenova, I., Polyakov, A., Gareev, A., Makarov, V., Kazakov, I., & Pesin, M. (2023). Machinability features of Ti-6Al-4V alloy with ultrafine-grained structure. Metals, 13(10), 1721. https://doi.org/10.3390/met13101721
- Suhaimey, M. D., Tamin, N., Salleh, K. M., Hakimi, A. A., Rashidi, I. F., Azlan, U. A. A., Ab Wahab, N., & Wan Abdul Malik, W. A. H. (2025). Optimisation of CNC turning parameters using RSM for Inconel 718 in dry cutting conditions, focusing on surface roughness. Journal of Mechanical Engineering,

- 22(3), 16-27. https://doi.org/10.24191/jmeche.v22i3.5318
- Tharazi, I., Sulong, A. B., Salleh, F. M., Abdullah, A. H., & Ismail, N. F. (2020). Application of response surface methodology for parameters optimization in hot pressing kenaf reinforced biocomposites. Journal of Mechanical Engineering, 17(3), 131–144. https://doi.org/10.24191/jmeche.v17i3.15318
- Tharazi, I., Rahaman, W. E. W. A., & Sarizam, M. I. E. (2024). Performance analysis of cutting glass fibre epoxy reinforced composites using an abrasive water jet machining process. International Journal of Integrated Engineering, 16(9), 273–283. https://doi.org/10.30880/ijie.2024.16.09.022
- Tripathi, D. R., Vachhani, K. H., Kumari, S., Dinbandhu, & Abhishek, K. (2019). Experimental investigation on material removal rate during abrasive water jet machining of GFRP composites. Materials Today: Proceedings, 26(2), 1389–1392. https://doi.org/10.1016/j.matpr.2020.02.280
- Umanath, K., Devika, D., & Rashia Begum, S. (2021). Experimental investigation of role of particles size and cutting passes in abrasive waterjet machining process on titanium alloy (Ti–6Al–4V) using Taguchi's method. Materials and Manufacturing Processes, 36(8), 936–949. https://doi.org/10.1080/10426914.2020.1866202
- Wang, H., Yuan, R., Zhang, X., Zai, P., & Deng, J. (2023). Research progress in abrasive water jet processing technology. Micromachines, 14(8), 1526. https://doi.org/10.3390/mi14081526